MDPI

Article

Optimal Placement and Capacity of BESS and PV in EV Integrated Distribution Systems: The Tenth Feeder of Phitsanulok Substation Case Study

Sirote Khunkitti [1,]*[iD], Natsawat Pompern [1], Suttichai Premrudeepreechacharn [1] and Apirat Siritaratiwat [2]

[1] Department of Electrical Engineering, Faculty of Engineering, Chiang Mai University, Chiang Mai 50200, Thailand; natsawat_pom@cmu.ac.th (N.P.); suttic@eng.cmu.ac.th (S.P.)
[2] Department of Electrical Engineering, Faculty of Engineering, Khon Kaen University, Khon Kaen 40002, Thailand; apirat@kku.ac.th
* Correspondence: sirote.khunkitti@cmu.ac.th; Tel.: +66-868-589-799

Abstract: Installing a battery energy storage system (BESS) and renewable energy sources can significantly improve distribution network performance in several aspects, especially in electric vehicle (EV)-integrated systems because of high load demands. With the high costs of the BESS and PV, optimal placement and capacity of them must be carefully considered. This work proposes a solution for determining the optimal placement and capacity of a BESS and photovoltaic (PV) in a distribution system by considering EV penetrations. The objective function is to reduce system costs, comprising installation, replacement, and operation and maintenance costs of the BESS and PV. The replacement cost is considered over 20 years, and the maintenance and operation costs incurred in the distribution system include transmission line loss, voltage regulation, and peak demand costs. To solve the problem, two metaheuristic algorithms consisting of particle swarm optimization (PSO) and the African vulture optimization algorithm (AVOA) are utilized. The tenth feeder of Phitsanulok substation 1 (PLA10), Thailand, which is a 91-bus distribution network, is tested to evaluate the performance of the proposed approach. The results obtained from the considered algorithms are compared based on distribution system performance enhancement, payback period, and statistical analysis. It is found from the simulation results that the installation of the BESS and PV could significantly minimize system cost, improve the voltage profile, reduce transmission line loss, and decrease peak demand. The voltage deviation could be reduced by 86%, line loss was reduced by 0.78 MW, and peak demand could be decreased by 5.706 MW compared to the case without BESS and PV installations.

Keywords: African vultures optimization algorithm; battery energy storage systems; distribution systems; electric vehicles; particle swarm optimization

1. Introduction

Currently, energy consumption is continuously rising because of economic expansion and developments in industrial technology, causing electricity to play a key role in boosting economies and raising the living standard in various countries [1–3]. In addition, the production and utilization of electric vehicles (EVs) and renewable energy, especially in photovoltaic (PV) industries, have increased, which will notably affect both the economy and the electricity production system in the future [4–8]. The growing number of EVs will require more electric vehicle charging stations, and the usage of PV, which will become common in daily life, will be integrated into electricity distribution systems, leading to risks in managing power systems from the perspective of the voltage profile and total harmonic distortion (THD) [9,10]. Therefore, to accommodate the increasing electricity demand from EVs and the growth of energy consumption, PV will be integrated into the distribution system, and energy storage systems (ESSs) will also be installed to preserve energy from

PV and the grid during times of low electricity demand and provide the energy back into the system during times of peak demand.

Various types of ESS technology have been studied to be efficiently installed in distribution systems selected based on a number of variables, including cost, energy capacity, efficiency, and reliability, with a primary focus on safety in operation [11]. Additionally, suitable ESSs to be installed in distribution networks should have a moderate discharge time frame (minutes to hours) since this discharge time frame can meet the daily load demands immediately, and battery energy storage systems (BESSs) mostly reach this time frame [12]. Moreover, by installing BESSs in distribution networks, the placement and capacity of the BESS must be considered as they are crucial factors in improving the efficiency and reliability of the distribution systems and reduce system costs. Due to the high price of the BESS, oversized BESSs may incur excessive investment costs with longer payback periods, and inappropriate BESS placement can incur large amounts of energy losses. With the optimal placement and capacity of the BESS, the remaining energy from DGs after being provided to the loads can be efficiently stored in the installed BESS with low power loss in the transmission lines, and the amount of stored energy is also appropriate to provide energy back to the system during high peak periods, resulting in peak shaving and voltage deviation reductions. So, the optimal placement and capacity of the BESS must be efficiently found to obtain the best feasible investment costs together with high system performance enhancement.

Many approaches have been introduced to find the optimal BESS location and sizing in distribution networks, and the optimal location and sizing of distribution generators (DGs) are also included in some literature. A novel algorithm called the artificial hummingbird algorithm (AHA) was introduced in [13] to find the best position and size of DGs based on biomass in radial systems, aiming to reduce losses and improve voltage deviation. The results indicated that the distribution system efficiency was improved in terms of reductions in power loss and voltage deviation. In [14], the best location and BESS sizing connected to renewable energy sources (RESs) were presented to find the minimum system cost in the IEEE 33-bus system. The genetic algorithm (GA) and particle swarm optimization (PSO) were used, and the results showed that PSO was more effective in cost reduction than GA. The best possible DG position and size in the 118-bus system of IEEE and the practical system in Egypt identified using a modified forensic-based investigation (mFBI) were introduced in [15]. The optimization problem has been considered a multi-objective function where the objective functions consist of minimizing energy loss, voltage deviation, and operation cost while maximizing voltage stability, and they demonstrated that mFBI outperformed various methods in the literature and generated better results according to the objective values. In [16], the GA and the greedy algorithm were applied to find the optimal position and size of a BESS connected to EVs and DGs to reduce installation, operation, and maintenance (O&M) costs in a rural 22-bus distribution network. In [17], the best feasible BESS installation combined with PV and wind turbine (WT) in the IEEE 33-bus distribution network was proposed, adopting the interior point method to control operations in conjunction with a distribution management system (DMS) and energy management system (EMS) aiming to decrease system expenses. It was found that BESS could enhance the performance of the system, as investigated through voltage deviation examination, power loss reduction, and peak demand decrease. In [18], a stand-alone microgrid system with 17 buses connected to residential loads and EVs was used to assess the best position and sizing of DGs and the BESS by applying teaching–learning-based optimization (TLBO), resulting in reduced power losses and improved voltage quality. The best BESS sizing and position in a radial distribution system were determined using the hierarchical planning mode and natural aggregation algorithm (NAA) in order to manage voltage and lower life cycle costs (LCC) [19]. The optimal installation of BESS utilizing a fuzzy method to forecast the ambiguity of load profiles and employing tabu search (TS) and simulated annealing (SA) to determine the DG capacity, battery quantity, BESS power, and BESS size and location was proposed in [20]. The results showed that the

presented methods could reduce purchased electricity costs from the grid and minimize power losses in the distribution system. As mentioned in previous works, it can be observed that various approaches have been introduced to find the optimal location and sizing of a BESS in distribution networks to minimize total system expenses comprising installation, replacement, power loss, voltage deviation, and peak demand costs. However, only some of these costs have been considered in each work, and most of these works applied traditional algorithms to solve the problems.

To fully and efficiently reduce system costs and improve distribution network performance, some studies have proposed approaches to find the optimal position and capacity of BESS in distribution networks by considering the total system costs, and some of them employed newly proposed algorithms to achieve efficient objective values. In [21], the best possible BESS installation alongside DGs and EVs was proposed, applying multi-objective PSO (MOPSO) and Monte Carlo simulation (MCS) to search for the optimal LCC, including initial investment costs (ICs), maintenance costs (MCs), and replacement costs (RCs). The outcomes indicated that installing the BESS in the distribution system reduced the total LCC. The optimal approach for Interline-PV (I-PV) systems under varying EV loads, focusing on reducing power losses and improving voltage profiles, was proposed in [22]. Three optimization algorithms were employed to specify the best solution strategies, and it was found that I-PV enhanced voltage profiles, reduced power losses, and was able to be adapted to practical problems. However, this work only evaluated the installation of I-PV, which included the installation of PV and a BESS at the same location, without considering the costs of installing the BESS and the optimal PV location. In [23], the best feasible BESS position and size in a DG-connected distribution system using GA, PSO, and the salp swarm algorithm (SSA) were proposed to reduce system expenses consisting of power loss, voltage fluctuation, and peak power expenses in the IEEE 33- and 69-bus systems. It revealed that system costs, power loss, and peak demand could be reduced and voltage stability could be improved. However, only the O&M costs of the system were computed in this research without considering installation and battery replacement costs. The best feasible placement and sizing of BESS in the IEEE 33- and 69-bus distribution networks connected to PV and EVs were presented in [24] to decrease the system expenses, consisting of installation, replacement, and O&M costs of the BESS, and the distribution network performance was improved in terms of transmission loss, the voltage deviation index (VDI), and peak power reductions. Three algorithms consisting of PSO, the African vulture optimization algorithm (AVOA), and SSA were applied to solve this problem and compared the aspects of the system cost, distribution system efficiency improvement, payback period, and statistical results, and the results in both systems showed that PSO gave the best objective values and AVOA provided the fastest payback period. A detailed summary of the previous work conducted in the optimal placement and capacity of the BESS is provided in Table 1.

Table 1. Summary of the previous works conducted in the optimal placement and capacity of the BESS.

Refs	Objective Functions	Total System Costs	DGs	Test Systems	Algorithms
[13]	minimizing losses and voltage deviation	x	biomass	IEEE 33-, 69-, 119-bus system	AHA
[14]	minimizing voltage regulation cost, power loss cost, and peak demand cost	x	PV, WT	IEEE 33-bus system	GA, PSO
[15]	minimizing energy loss, voltage deviation, operation cost while maximizing voltage stability	x	PV, WT	Egypt system	mFBI
[16]	minimizing investment and O&M costs	✓	PV	rural 22-bus network	GA, greedy algorithm

Table 1. *Cont.*

Refs	Objective Functions	Total System Costs	DGs	Test Systems	Algorithms
[17]	minimizing battery costs and system costs due to system losses, peak demand, and voltage regulation.	✓	PV, WT	IEEE 33-bus system	interior point method
[18]	minimizing power losses and improving voltage quality	x	PV, WT,	17-bus stand-alone microgrid	TLBO
[19]	minimizing investment cost, operation cost, maintenance cost, and residual value	x	PV	IEEE 15-, 69-bus system	NAA
[20]	minimizing operation cost and reliability cost	x	N/A	modified 21-node system	TS, SA
[21]	minimizing life cycle cost including initial, maintenance, and replacement costs	✓	PV, WT	a house in Sanandaj	MOPSO, MCS
[22]	minimizing power losses and improving voltage quality	x	PV	IEEE 33-bus system system	COA, PSO, GWO
[23]	minimizing reduce system costs consisting of power loss, voltage deviation, and peak demand costs	x	PV, WT	IEEE 33-, 69-bus system	GA, PSO, SSA
[24]	minimizing system costs consisting of installation, replacement, and O&M costs	✓	PV	IEEE 33-, 69-bus system	PSO, SSA, AVOA

Although some research studies have investigated the optimal position and capacity of BESS, most of them have not evaluated installation and battery replacement costs [22,23]. In [24], the installation and battery replacement costs were included; however, the location and size of PV have not been optimally placed, and only IEEE systems were tested. Moreover, it was found in [24] that PSO and AVOA were high-performance algorithms to solve the problem of the optimal position and sizing of BESSs in distribution systems connected to PV and EVs. Therefore, the optimal placement and capacity of the BESS and PV in distribution networks considering EV penetrations are proposed in this work. The objective functions considered to be minimized are system costs including installation, replacement, and O&M costs of the BESS and the installation cost of PV, and the network performance is aimed to be improved in aspects of line loss, voltage deviation, and peak demand reductions by the BESS installation. A practical system, namely the tenth feeder of Phitsanulok substation 1 (PLA10), Thailand, which is a 91-bus distribution system, is used to evaluate the performance of the approach. The conventional efficient algorithm, which is PSO, as well as the new efficient algorithm, which is AVOA, are utilized to determine the optimal solutions.

The main contributions of this work are as follows:

1. The optimal placement and capacity of the BESS and PV in the PLA10 distribution system considering EV penetrations are investigated in this work by considering the overall system costs including installation, replacement, and operational and maintenance costs as the objective functions to be minimized.
2. The distribution system performance is improved by reducing line losses, minimizing peak demand, and enhancing the voltage profile after the installation of the BESS and PV.
3. Two optimization algorithms including PSO and AVOA are employed to find the optimal solutions, and their simulation results, statistical analysis, and payback period are compared.

The rest of the paper is divided as follows. Section 2 introduces input data models of the BESS and EV charging stations in the distribution network. The problem formulation of the optimal placement and capacity of the BESS and PV in the distribution network is provided in Section 3. In Section 4, the methodology of this work is presented. Section 5 shows the simulation results and discussions. Finally, the conclusion of this work is presented in Section 6.

2. Input Data Models

This section presents the modeling of the BESS and EV charging stations in the distribution network.

2.1. Battery Energy Storage Systems (BESSs) in a Distribution System

An electrochemical BESS is employed in this paper since it has an appropriate discharge time and the ability to quickly respond to daily loads [12,25–27]. The simulation of the BESS is explained below.

2.1.1. BESS Simulation

A Li-ion battery has been selected as the BESS of this work due to its various advantages, including over 90% efficiency, high energy density (90–190 Wh/kg), high life cycle, and reasonable cost. Although Li-ion has some disadvantages such as the need for a protection circuit, degradation at high temperatures and high voltage, and the impossibility of rapid charge at freezing temperatures when compared to other BESSs, Li-ion can still overcome other BESSs for this work because of its various advantages and suitability for distribution systems. However, the temperature, number of BESS operation cycles, and depth of discharge (DOD) are some of the factors that can impact the life cycle of a Li-ion battery. So, extended service life of the BESS is achieved by controlling heat dissipation at the ideal temperature, which is between 15 and 35 degrees Celsius, preventing frequent charging and discharging, and maintaining operation at the recommended DOD of a Li-ion, which is 80% of the total capacity [28,29].

The BESS simulation considers charging and discharging the BESS for the same amount of time each day, or 24 h [14,17,23]. The period is divided evenly into one hour, thirty minutes, and fifteen minutes to accommodate the battery's charging and discharging rates of 24, 48, or 96, respectively. The charging and discharging rates over any period are calculated using the given equation.

$$C_{iT} = \begin{bmatrix} E_B(1) \\ \vdots \\ E_B(m) \end{bmatrix} \tag{1}$$

where C_{iT} is the charging and discharging rates in the considered duration $E_B(t)$ is the energy in the BESS (MWh) at time $t = 1, 2, 3, \ldots, m$.

To calculate the energy in the BESS, the Fourier series is applied using the Fourier coefficient vector (C_{iF}), produced by the optimization operation since the energy in the BESS represented in finely dispersed periodic patterns can be found by using the Fourier series. The periodic pattern is separated into sinusoidal components in the time domain using the Fourier series, which allows for a comprehensive analysis of the BESS energy [30]. In this method, the process uses the Fourier transform to forecast the energy (E_B) in the BESS hourly, starting at random with sixteen values of the Fourier coefficient. Then, the state of energy (SOE) is represented for the whole period considered by using the Fourier series. The energy in the BESS is calculated using the given equations [17,30].

$$C_{iF} = \begin{bmatrix} a_1, b_1 \\ \vdots \\ a_n, b_n \end{bmatrix} \tag{2}$$

$$E_B(t) = a_0 + a_1 \cos\left(\frac{2\pi t}{T}\right) + b_1 \sin\left(\frac{2\pi t}{T}\right) + \ldots + a_n \cos\left(\frac{2\pi n t}{T}\right) + b_n \sin\left(\frac{2\pi n t}{T}\right) \quad (3)$$

where a_0, a_n, b_n, n, t, and T denote the constant Fourier coefficient, Fourier cosine coefficient, Fourier sine coefficient, number of Fourier coefficients, which is set to 8, time, and total period, respectively. Additionally, a_n and b_n are optimization variables in this problem.

By substituting C_{iF} from Equation (2) into Equation (3), the BESS energy, $E_B(t)$, can be found. According to Equation (3), a_0 is not required because it has no effect on the BESS charging and discharging processes and the energy cost coefficient. Thus, following an optimization process, it may be adjusted to guarantee that the BESS power curve does not fall below the minimal amount necessary to meet the DOD criteria. The changes in energy in the BESS at two continuous times can be calculated using Equation (4), and it is used to determine the BESS power as in Equation (5) and Equation (6). The BESS power is utilized to present the state of the BESS. The BESS power is positive when it is in a charging state, signifying the addition of energy to the BESS. On the other hand, the BESS power is negative when it is in the discharging stage, signifying the release of energy from the BESS.

$$\Delta E_B = E_B(t) - E_B(t-1) \tag{4}$$

$$P_B(t) = \Delta E_B / (\Delta t \times \eta_c), P_B(t) > 0 \tag{5}$$

$$P_B(t) = (\Delta E_B \times \eta_d) / \Delta t, P_B(t) < 0 \tag{6}$$

where ΔE_B indicates the changes in energy in the BESS at two continuous times, η_c, η_d, P_B, and Δt are the charging efficiency of the BESS, discharging efficiency of the BESS, BESS power, and sampling interval time, respectively, $\eta_c = \eta_d = \sqrt{\eta_{bat}}$, and η_{bat} is the cycle efficiency of BESS, which is set to 0.9.

2.1.2. BESS Simulation

Power and energy capacities should be considered to find the optimal BESS capacity in order to reduce overall costs and maintain the reliability and quality of a distribution system. The number of cycles and the SOC, which are two main factors affecting the BESS life, should also be considered [11]. The efficiency of the BESS life cycle can be increased by reducing daily SOC fluctuations via improved charging and discharging cycles in the BESS. Thus, the BESS size can be formulated as given in Equation (7). The daily cycle and lifespan of the BESS are evaluated as Equations (8) and (9), respectively.

$$Battery\ size(\text{kWh}) = \frac{\left|E_B^{\max} - E_B^{\min}\right|}{DOD_{\max}} \tag{7}$$

where $E_B^{\max}$ and $E_B^{\min}$ are the maximum and minimum energies of the BESS, respectively, and $DOD_{\max}$ is the maximum DOD, which is equal to 0.8 in this work.

$$Cycles = \frac{1}{2}\left(\frac{\sum_{t=1}^{T} E_B(t) - E_B(t-1)}{DOD_{\max} \times Battery\ size}\right) \tag{8}$$

$$Q\ (\text{years}) = \frac{CyclesLife}{Cycles \times D} \tag{9}$$

where *Cycles* indicate the daily cycle of the BESS, D is operation days, which is equal to 285 days, *CyclesLife* is the nominal life cycle of the Li-ion battery, which is 3000 cycles, and Q represents the lifespan of the BESS in years.

2.2. Charging Station for EV Modeling

To find the best possible location and sizing of the BESS and PV in the distribution network connected to EV charging stations, the charging stations are considered EV penetrations. To add the EV penetration into the systems, it can be assumed that the BESS

and grid feed power to the EVs according to the penetration load while increasing the EV demand on all buses through the use of an AC/DC converter or charging port. [22,31]. Additional active and reactive loads of EVs are calculated using the presented equations.

$$P^0_{ev(n)} = \lambda_{ev} \times P^0_{L(n)} \tag{10}$$

$$Q^0_{ev(n)} = P^0_{ev(n)} \times \tan(\varphi_{n(c)}) \tag{11}$$

where $P^0_{ev(n)}$ and $Q^0_{ev(n)}$ are additional active and reactive loads by the EV penetrations at the nth bus, λ_{ev} is a scale factor that shows how much of an EV load there is in relation to the real power demand at each location, $P^0_{L(n)}$ is the nominal real load power at the nth bus, and $\varphi_{n(c)}$ is the AC/DC converter power factor.

The total active and reactive load powers of the EV penetration at each placement are then formulated using the provided equations.

$$P^t_{d(n)} = P^0_{L(n)} \times \left(\frac{V^t_{(n)}}{V^0_{(n)}}\right)^{\alpha} + \left\{ P^0_{ev(n)} \times \left(\frac{V^t_{(n)}}{V^0_{(n)}}\right)^{\alpha_{ev}} \right\} \tag{12}$$

$$Q^t_{d(n)} = Q^0_{L(n)} \times \left(\frac{V^t_{(n)}}{V^0_{(n)}}\right)^{\beta} + \left\{ Q^0_{ev(n)} \times \left(\frac{V^t_{(n)}}{V^0_{(n)}}\right)^{\beta_{ev}} \right\} \tag{13}$$

where $P^t_{d(n)}$ and $Q^t_{d(n)}$ are the total active and reactive power loads integrating the EV penetration at the nth bus, respectively, $Q^0_{L(n)}$ is the nominal reactive load power at bus n, $V^t_{(n)}$ and $V^0_{(n)}$ indicate the time and initial nominal voltages, respectively, α and β are active and reactive power exponents of the load demand, respectively, which are both equal to 0, and α_{ev} and β_{ev} are the active and reactive power exponents of the EV load demand, respectively, which are equal to 2.59 and 4.06, respectively [31].

3. Problem Formulation

The optimal position and sizing of the BESS and PV in the distribution network integrated with EV charging stations in this research are proposed to minimize the system costs comprising the installation, replacement, and operation and maintenance costs of the BESS and installation cost of the PV. The system costs are set to be the minimized objective function subject to technical constraints. So, this section defines the objective function and constraints of this work.

3.1. Objective Function

The system costs are considered the objective function to minimize the costs of the BESS installation, which are the investment cost, replacement cost, and operation and maintenance costs and the cost of the PV installation [18,19,23]. The objective function is determined using the equations below.

$$f(C_{iF}) = \min(C_{system}) \tag{14}$$

$$C_{system} = C_I + C_R + C_{O\&M} + C_{pv} \tag{15}$$

$$C_I = N_{bat} \times \gamma_I \tag{16}$$

$$C_R = N_{bat} \times \gamma_I \times \frac{t_{year}}{Q(years)} \tag{17}$$

$$C_{O\&M} = C_{VR} + C_{loss} + C_p \tag{18}$$

$$C_{VR} = \left(\sum_{t=1}^{T} \sum_{i=1}^{N_{bus}} \left| V_i - V_{ref} \right| \right) \times \gamma_{VR} \tag{19}$$

$$C_{loss} = \left(\sum_{t=1}^{T} \sum_{i=1}^{N_{br}} |P_L| \right) \times \gamma_{loss} \tag{20}$$

$$C_p = P_{\max} \times \Delta t \times \gamma_p \tag{21}$$

$$C_{pv} = N_{pv} \times \gamma_{pv} \tag{22}$$

where C_{system}, C_I, C_R, $C_{O\&M}$, and C_{PV} are the system costs, BESS investment cost, BESS replacement cost, BESS operation and maintenance costs, and PV installation cost, respectively; C_{VR}, C_{loss}, and C_p are the costs of voltage regulation, line loss, and peak demand, respectively; N_{bat}, N_{pv}, t_{year}, V_i, V_{ref}, P_L, and P_{max} are the BESS size (kWh), PV size (kW), study duration (set to 20 years), voltage at the ith bus (p.u.), reference voltage, which is 1 p.u., real loss in each line, and maximum power demand, respectively; N_{bus}, N_{br}, γ_I, γ_{VR}, γ_{loss}, γ_p, and γ_{pv} are the total number of buses, total number of branches, rate of the BESS installation cost (equal to 100 \$/kWh), rate of the voltage regulation cost (equal to 0.142 \$/p.u.), rate of the transmission loss cost (equal to 0.284 \$/kWh), rate of the maximum energy demand cost (equal to 200 \$/kWh/year), and rate of the PV installation cost (equal to 2000 \$/kW), respectively.

When integrating the BESS into the distribution system, THD can occur when the power from the BESS is transmitted through the power conversion system (PCS). The THD can cause the voltage and current waveforms to be distorted resulting in low-quality transmitted power. However, most of the present distribution systems normally contain high-efficiency filters in the PCS, which can significantly relieve THD. So, by integrating the BESS into distribution systems, THD is assumed to be ignored in this work.

3.2. Constraints

The considered objective function must be subjected to technical constraints while solving the optimization problem. The equality and inequality constraints of this work are presented below.

3.2.1. Equality Constraints

The system power balance in the distribution system is controlled as presented in the given equation.

$$P_{grid}(t) = P_D(t) - P_{pv}(t) \pm P_B(t) + P_L(t) \tag{23}$$

where $P_{grid}(t)$, $P_D(t)$, $P_{pv}(t)$, $P_B(t)$, and $P_L(t)$ are the power of the grid, power of the load demand, power of the PV, power of the BESS, and power of the transmission loss at time t, respectively.

3.2.2. Inequality Constraints

The voltages of all buses must be within the range of the limits, which is considered $\pm 10\%$ of the reference voltage as shown in the following Equation.

$$V_{\min} \leq V_i^t \leq V_{\max} \tag{24}$$

where $V_{\min}$ and $V_{\max}$ indicate the minimum and maximum voltages of each bus, which are 0.9 and 1.1, respectively, and V_i^t is the voltage at bus i at time t.

The BESS power and energy are also restricted to keep it safe while charging and discharging. These constraints are represented by the provided equations.

$$P_B^{\min} \leq P_{cha}^t, P_{dis}^t \leq P_B^{\max} \tag{25}$$

$$E_B^{\min} \leq E_B^t \leq E_B^{\max} \tag{26}$$

where $P_B{}^{min}$ and $P_B{}^{max}$ denote the minimum and maximum powers of the BESS, respectively, $P^t{}_{cha}$ and $P^t{}_{dis}$ are the charging and discharging of the BESS at time t, and $E_B{}^{min}$ and $E_B{}^{max}$ are the minimum and maximum energies of the BESS, respectively.

4. Methodology

To solve the optimization problem in this work, metaheuristic algorithms, namely PSO and AVOA, are applied to provide the optimal location and sizing of the BESS and PV in the distribution network. Moreover, these algorithms are compared using the distribution system efficiency evaluation in aspects of VDI, line losses, and peak demand enhancement. The methodology used in this work is explained below.

4.1. Particle Swarm Optimization (PSO)

PSO was introduced by Kennedy and Eberhart in 1995 to determine the optimal solution to an optimization problem. Despite being a traditional approach, PSO has shown the potential to outperform recently proposed optimization algorithms in various studies [23,32,33]. Moreover, PSO was considered a high-performance algorithm in solving the problem of finding the placement and location of the BESS in distribution networks as presented in [24]. A key idea of PSO came from imitating a flock of birds foraging for food. Each bird in the flock would follow the bird that is currently closest to the best food source [34]. Every particle in the PSO, which is each bird in the flock, represents a potential solution, and the best solution can be searched for using the PSO process. The process of PSO can be explained by updating the velocity and position of each particle using the equations below.

$$v_i^{k+1} = w^k \times v_i^k + c_1 r_1 (p_{best,i}^k - x_i^k) + c_2 r_2 (g_{best}^k - x_i^k) \tag{27}$$

$$x_i^{k+1} = x_i^k + v_i^{k+1} \tag{28}$$

where v_i^{k+1} and v_i^k denote the velocity of particle i at iterations $k + 1$ and k, respectively, w^k is the inertia weight at iteration k, c_1 and c_2 are positive constant values, r_1 and r_2 refer to random values between 0 and 1, $p^k{}_{best,i}$ and $g^k{}_{best}$ are the best position of the particle i (personal best) and the best position of the entire particle (global best) at iteration k, respectively, and the positions of particle i at iterations k and $k + 1$ are indicated by x_i^k and x_i^{k+1}, respectively. w^k can be calculated using the following equation.

$$w^k = w_{max} - \left(\frac{w_{max} - w_{min}}{iter_{max}} \times k \right) \tag{29}$$

where w_{max} and w_{min} are the maximum and minimum inertia weights set to 0.9 and 0.4, respectively, and $iter_{max}$ is the maximum iteration.

4.2. African Vulture Optimization Algorithm (AVOA)

African vultures, which normally migrate in groups to search for food and settle down where the food source is, which refers to the optimal solution, served as the model for the new metaheuristic algorithm called AVOA. The initial locations of the vultures in the search space are randomly sampled to start the AVOA, and the equation below is used to determine the best two vultures.

$$R(i) = \begin{cases} BestVulture_1 \ if \ p_i = L_1 \\ BestVulture_2 \ if \ p_i = L_2 \end{cases} \tag{30}$$

$$p_i = \frac{F_i}{\sum_{i=1}^n F_i} \tag{31}$$

where $R(i)$ denotes one of the best vultures chosen, p_i indicates the probability of selecting the best solution, the indicators determined before the searching process are represented by

L_1 and L_2 where the values are between 0 and 1 and the summation of them must equal 1, and n is the number of vulture groups. Then, the starvation rates of both vultures can be found using the provided equations.

$$F = (2 \times rand_1 + 1) \times z \times \left(1 - \frac{iter}{iter_{\max}}\right) + t \tag{32}$$

$$t = h \times \left(\sin^w\left(\frac{\pi}{2} \times \frac{iter}{iter_{\max}}\right) + \cos\left(\frac{\pi}{2} \times \frac{iter}{iter_{\max}}\right) - 1\right) \tag{33}$$

where F is the starvation rate of the vultures, $rand_1$ refers to a random value between 0 and 1, z is a number randomly generated between -1 and 1, which is regenerated in each iteration, t is a parameter used to enhance the searching operation, h indicates a number randomly chosen between -2 and 2, and the exploration and exploitation phases can be balanced by using w [35]. If a number generated by z is less than 0 ($[-1, 0)$), the vultures are starved, and if a number generated by z is more than 0 ($[0, 1]$), the vultures are satiated. The starvation rate of the vultures can be described as shown below.

If the F of the vultures is equal to or less than 1, the vultures are satiated. Then, at random distances from one of the two groups, the vultures explore for food by updating the position as shown in the given equations.

$$D(i) = |X \times R(i) - P(i)| \tag{34}$$

$$P(i + 1) = R(i) - D(i) \times F \tag{35}$$

$$P(i + 1) = R(i) - F + rand_2 \times ((ub - lb) \times rand_3 lb) \tag{36}$$

where $D(i)$ is adopted to update the best vulture positions in two groups, X is the movement of vultures that randomly move to protect food from others, $P(i)$ and $P(i + 1)$ are the vectors of the vulture position at iterations i and $i + 1$, $rand_2$ and $rand_3$ are numbers randomly generated between 0 and 1, and ub and lb are the variable upper and lower bounds, respectively.

When F is equal to or more than 0.5 and less than 1, violent arguments break out among vultures, and hostile vultures do not share their food. Weaker vultures obtain food scraps from stronger vultures. So, the vultures update their positions in this situation using the presented equations.

$$d(t) = R(i) - P(i) \tag{37}$$

$$P(i + 1) = D(i) \times (F + rand_4) - d(t) \tag{38}$$

$$S_1 = R(i) \times \left(\frac{rand_5 \times P(i)}{2\pi}\right) \times \cos(P(i)) \tag{39}$$

$$S_2 = R(i) \times \left(\frac{rand_6 \times P(i)}{2\pi}\right) \times \sin(P(i)) \tag{40}$$

$$P(i + 1) = R(i) - (S_1 + S_2) \tag{41}$$

where $d(t)$ denotes the distance of the vulture from one of the best vultures in the two groups, S_1 and S_2 are spiral equations obtained between all vultures and one of the best vultures in the two groups, and $rand_4$, $rand_5$, and $rand_6$ are numbers randomly generated between 0 and 1.

Conflicts occur among vultures if F is less than 0.5 because it is assumed that there are a greater number of vultures than food sources. Usually, all vultures tend to fly to the same place where the food is. Thus, the vulture position is updated using the equations shown below.

$$A_1 = BestVulture_1(i) - \frac{BestVulture_1(i) \times P(i)}{BestVulture_1(i) - P(i)^2} \times F \tag{42}$$

$$A_2 = BestVulture_2(i) - \frac{BestVulture_2(i) \times P(i)}{BestVulture_2(i) - P(i)^2} \times F \tag{43}$$

$$P(i+1) = \frac{A_1 + A_2}{2} \tag{44}$$

$$P(i+1) = R(i) - |d(t)| \times F \times Levy(d) \tag{45}$$

where A_1 and A_2 are rivalries for food that might lead to an accumulation of different vulture species in one food supply, the best vultures of the first and second groups at iteration i are represented by $BestVulture_1(i)$ and $BestVulture_2(i)$, respectively, and $Levy(d)$ indicates a Levy flight employed to boost the randomness of AVOA and is calculated using the presented equation.

$$Levy(d) = 0.01 \times \frac{u \times \sigma}{|v|^{\frac{1}{\beta}}}, \sigma = \left(\frac{\Gamma(1+\beta) \times \sin(\frac{\pi\beta}{2})}{\Gamma(1+2\beta) \times \beta \times 2(\frac{\beta-1}{2})} \right)^{\frac{1}{\beta}} \tag{46}$$

4.3. System Efficiency Evaluation

After the installation of the BESS and PV, the efficiency of the distribution network is investigated regarding different aspects by referring to the objective function in terms of VDI, transmission losses, and peak demand.

4.3.1. Voltage Deviation Index (VDI)

The efficiency of the distribution network is evaluated using the VDI to examine the voltage profile improvement after the BESS and PV installations. The percentage of VDI is found by the difference between the reference voltage and the actual voltage for each period as the presented equation.

$$\%VDI_i = \max_T \frac{|V_{ref} - V_i|}{V_{ref}} \times 100,$$

$$\%VDI = \sum_{i=1}^{N_{bus}} \%VDI_i \tag{47}$$

where $\%VDI_i$ is the maximum percentage of VDI at bus i for each period T, V_{ref} and V_i are the voltage values of the reference bus and bus i, respectively, $\%VDI$ is the total percentage of the VDI in the system, and N_{bus} is the number of buses.

4.3.2. Transmission Losses

After installing the BESS and PV, the distribution network's efficiency is also assessed and compared using transmission losses, which are calculated using the following equation and comprise active power, reactive power, and apparent power losses.

$$P_{loss} = \sum_{t=1}^{T} \sum_{l}^{N_{br}} P_L^t,$$

$$Q_{loss} = \sum_{t=1}^{T} \sum_{l}^{N_{br}} Q_L^t,$$

$$S_{loss} = \sqrt{P_{loss}^2 + Q_{loss}^2} \tag{48}$$

where P_{loss}, Q_{loss}, and S_{loss} indicate the active power, reactive power, and apparent power losses, respectively, for each period T, and the active and reactive power losses of line l at each time t are represented by P^t_L and Q^t_L, respectively.

4.3.3. Peak Demand

Peak demand is evaluated after the installation of the BESS and PV specified by peak shaving. The peak demand, which considers a duration of 24 h in this work, is the maximum active power consumption under the consideration period.

4.4. Implementation

The placement and sizing of the BESS and PV in the distribution network considering EV penetrations are optimized by employing two metaheuristic algorithms comprising PSO and AVOA. The optimization process of the proposed approach is illustrated by the flowchart in Figure 1.
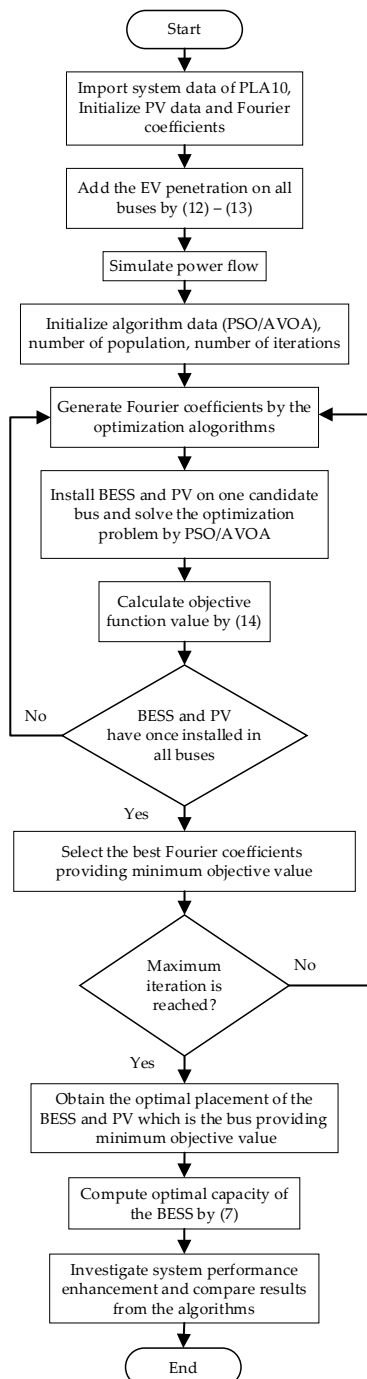
Figure 1. Optimization process of the proposed approach.

5. Simulation Results

The optimal placement and sizing of the BESS and PV were simulated in the practical distribution network by considering EV penetrations. The two algorithms, which are PSO and AVOA, were used to generate the solutions to the optimization problem with minimum system costs. The process was operated in MATLAB 2021a, and MATPOWER 7.1 was adopted to simulate the power flow [36]. The population number and maximum iterations of the metaheuristic algorithms were set to 60 and 250, respectively. The input system data and simulation results are presented and discussed in the following subsections.

5.1. Input System Data

The practical distribution network investigated in this study is the tenth feeder of Phitsanulok substation 1 (PLA10), Thailand, which is a 91-bus distribution network. At present, the Provincial Electricity Authority of Thailand is planning to install BESSs in several substations due to the increasing load demands, renewable energy sources, and EVs. Phitsanulok is an important economic zone of the upper central region of Thailand (the capital city of Thailand is in the central region), and there will be more investment in this area in the future. So, by installing a BESS and PV in Phitsanulok Substation, the growing load demands and EV demands will be able to be fully supported, and the system performance will be significantly enhanced in the future. The single-line diagram of PLA10 is shown in Figure 2, and the system data including load demand at each bus and transmission line data are given in Table A1 in Appendix A. The base power is 1 MVA, the base voltage is 22 kV, and the maximum load demand of the system is 9045.40 kW. The 24-h load demand and PV generation are presented in p.u. as shown in Table 2. The load demand and EV penetration at 20%, 40%, and 60% of the PLA10 distribution network within a day are illustrated in Figure 3.
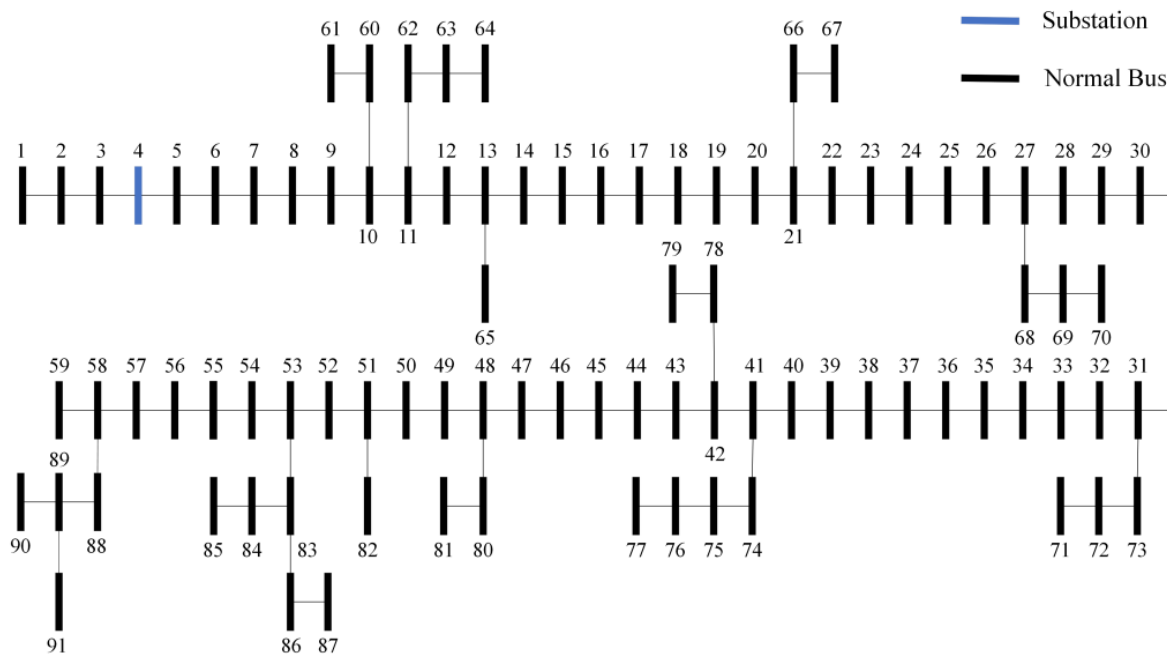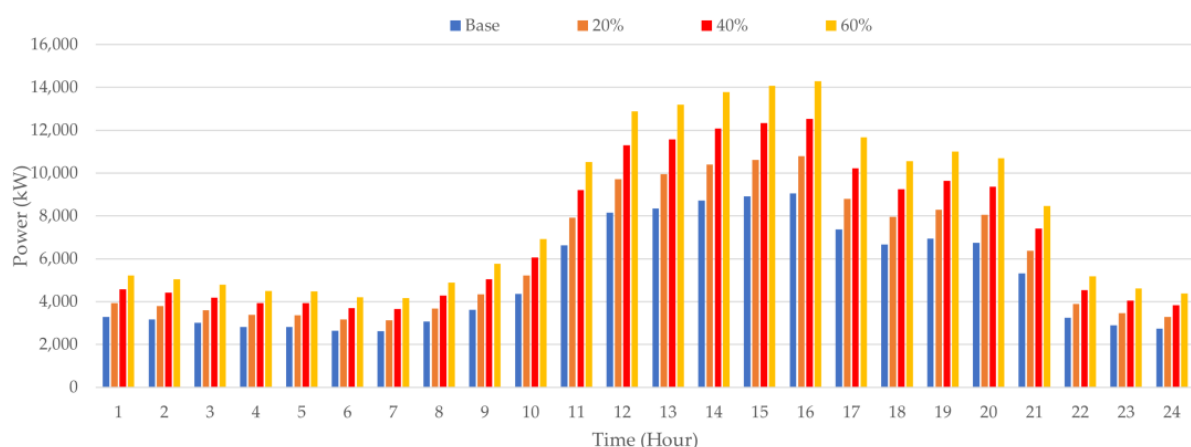
Figure 2. Single-line diagram of the PLA10 distribution network.

Table 2. Hourly load demand and PV generation within a day.

Hr.	Load (p.u.)	PVp (p.u.)	Hr.	Load (p.u.)	PVp (p.u.)
1	0.366	0.000	13	0.923	0.987
2	0.353	0.000	14	0.964	0.916

Table 2. *Cont.*

Hr.	Load (p.u.)	PVp (p.u.)	Hr.	Load (p.u.)	PVp (p.u.)
3	0.335	0.000	15	0.985	0.729
4	0.315	0.000	16	1.000	0.427
5	0.314	0.000	17	0.817	0.179
6	0.295	0.000	18	0.739	0.014
7	0.292	0.072	19	0.770	0.000
8	0.342	0.325	20	0.748	0.000
9	0.404	0.608	21	0.592	0.000
10	0.485	0.820	22	0.363	0.000
11	0.736	0.950	23	0.323	0.000
12	0.902	1.000	24	0.306	0.000

Figure 3. Hourly load demand and EV penetration at 20%, 40%, and 60% of the PLA10 distribution network.

5.2. Results and Discussion

The optimal position and sizing of the BESS and PV were generated by the considered algorithms in the PLA10 distribution network. After the installation of the BESS and PV, the effectiveness of each algorithm is examined in terms of the minimal system costs, which include the costs of the PV installation and operation and maintenance as well as the investment and replacement costs. Furthermore, the performance improvement of the distribution network generated by PSO and AVOA is compared before and after BESS and PV installation in aspects of the VDI, line loss, and peak demand. The simulation results of this system are presented as follows:

5.2.1. Optimal Placement and Capacity of the BESS and PV

To find the most feasible placement and capacity of the BESS and PV, the generated Fourier coefficients of the algorithms were used to calculate the SOE of the BESS in a day. The SOE depending on the load demand at each EV penetration throughout the day is illustrated in Figure 4. The optimal placement and capacity of the BESS and PV, power and lifetime of the BESS, and system costs are presented in Table 3.

From Figure 4, it can be noted from all EV penetrations that the BESS was in the charging state when the demand was low from 1 a.m. to around noon. Even though the demand started to become higher from 9 a.m. to noon, the BESS could still be in a charging state because of the energy generated from PV. The BESS then started to be in a discharging state in the afternoon until around 9 p.m. due to very high load demand. In Table 3, it is observed that the optimal placements of the BESS installation obtained by PSO were at the 41st bus at all considered EV penetrations and by AVOA at the 41st, 31st, and 41st buses at 20%, 40%, and 60% EV penetrations, respectively. By considering the objective function

value, PSO could provide better system costs than those of AVOA for all EV penetrations. So, by considering the results provided by PSO, the optimal placement was the 41st bus, which is the location of New Ice Factory, Ban Krang Subdistrict, Mueang Phitsanulok District, Phitsanulok. This place was observed and found to be suitable and has space to install the BESS. Furthermore, the optimal locations of the PV obtained by PSO were at the 51st bus at all EV penetrations. Unfortunately, the actual area survey found that this place cannot invest in PV installation since a university is located on this bus. However, the PV can be installed on a nearby bus, which is the 52nd bus, because there are areas that have not yet been developed. In addition, the largest BESS size obtained by PSO was 24.5914 MWh at 60% of EV penetrations, followed by AVOA, which was 24.5594 MWh at 40% of EV penetrations.
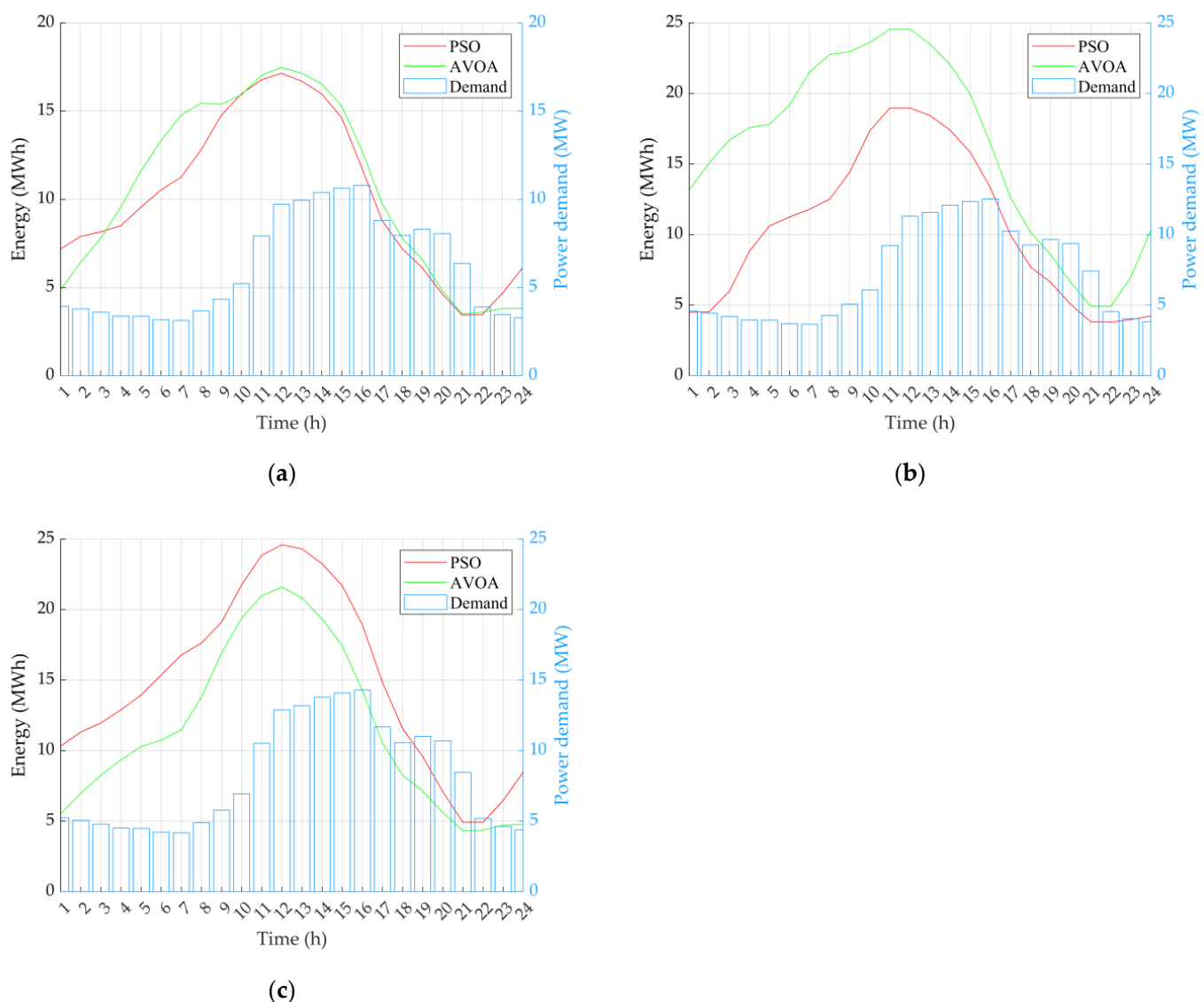
Figure 4. Stage of Energy (SOE) of the BESS generated by each algorithm and power demand in the PLA10 distribution system: (**a**) at λ_{ev} 20%; (**b**) at λ_{ev} 40%; (**c**) at λ_{ev} 60%.

Table 3. Optimal placement and capacity of the BESS and PV generated by each algorithm at each considered EV penetration.

Algorithm	λ_{ev}	BESS Placement	BESS Size (MWh)	PV Placement	PV Size (kW)	Power of BESS (MW)	Lifetime of BESS	System Costs ($)
PSO	20%	41	17.1415	51	2356.65	2.8215	8.824658	40,208,157.04
	40%	41	18.9705	51	2544.36	3.1765	8.824658	47,213,163.04
	60%	41	24.5914	51	3913.34	3.8928	8.824658	54,148,223.67
AVOA	20%	41	17.4733	51	2598.12	2.8497	8.784056	40,283,138.35
	40%	31	24.5594	82	2460.39	3.6452	8.824658	47,234,023.75
	60%	41	19.7769	50	3689.10	3.4387	8.824658	54,435,077.17

5.2.2. System Performance Improvement Comparison

The performance improvement of PLA10 was evaluated in different terms by referring to the objective function in terms of the VDI, transmission line losses, and peak demand before and after the installation of the BESS and PV by each algorithm as shown in Table 4, where the base case was the case without a BESS.

Table 4. Comparison of distribution system performance improvements before and after the BESS and PV installations.

Algorithm	λ_{ev}	VDI (%)	Real Power Loss (MW)	Reactive Power Loss (MVAr)	Apparent Power Loss (MVA)	Peak Demand (MW)
Base	20%	256.99	1.515	3.256	3.591	10.786
	40%	298.12	2.045	4.397	4.849	12.535
	60%	339.84	2.661	5.722	6.31	14.293
PSO	20%	199.77	1.126	2.434	2.682	6.882
	40%	233.55	1.546	3.341	3.681	8.171
	60%	253.81	1.881	4.064	4.478	8.587
AVOA	20%	197.60	1.125	2.432	2.679	6.749
	40%	242.57	1.570	3.398	3.743	7.749
	60%	261.65	1.921	4.153	4.575	9.143

It is observed from Table 4 that after the BESS and PV installations in the PLA10 distribution system, both algorithms provided reductions in the VDI, line losses, and peak demand for all EV penetrations. Moreover, it was found that AVOA was more efficient than PSO at 20% of EV penetration for VDI, losses, and peak demand reductions, but PSO generated better reductions of those terms than AVOA at 40% and 60% of EV penetrations except for the peak demand at 40% of EV penetration. The VDI could be reduced the most compared to the base case by around 59.39%, 64.57%, and 86.03% for 20%, 40%, and 60% of EV penetrations, respectively. The biggest decrease in real power loss compared to the base case reached approximately 0.39, 0.499, and 0.78 MW for 20%, 40%, and 60% of EV penetrations, respectively. For the highest peak demand reductions at 20%, 40%, and 60% of EV penetrations, they dropped around 4.037, 4.786, and 5.706 MW, respectively. So, the system performance could be significantly improved after the BESS and PV installations, especially in the high EV penetration case.

The 24-h voltage profiles at the weakest bus, which is the 91st bus, for 20%, 40%, and 60% of EV penetrations obtained by PSO and AVOA are presented in Figure 5 to show the improvement voltage profiles before and after the BESS and PV installations.

In Figure 5, it is noticeable that the voltage before the BESS and PV installations in the base case at 4.00 p.m. was at the lowest value because this period has the highest demand. However, the all-day voltage profile could be enhanced by installing the BESS and PV regardless of the increase in EV penetrations.

(**a**)

(**b**)

(**c**)
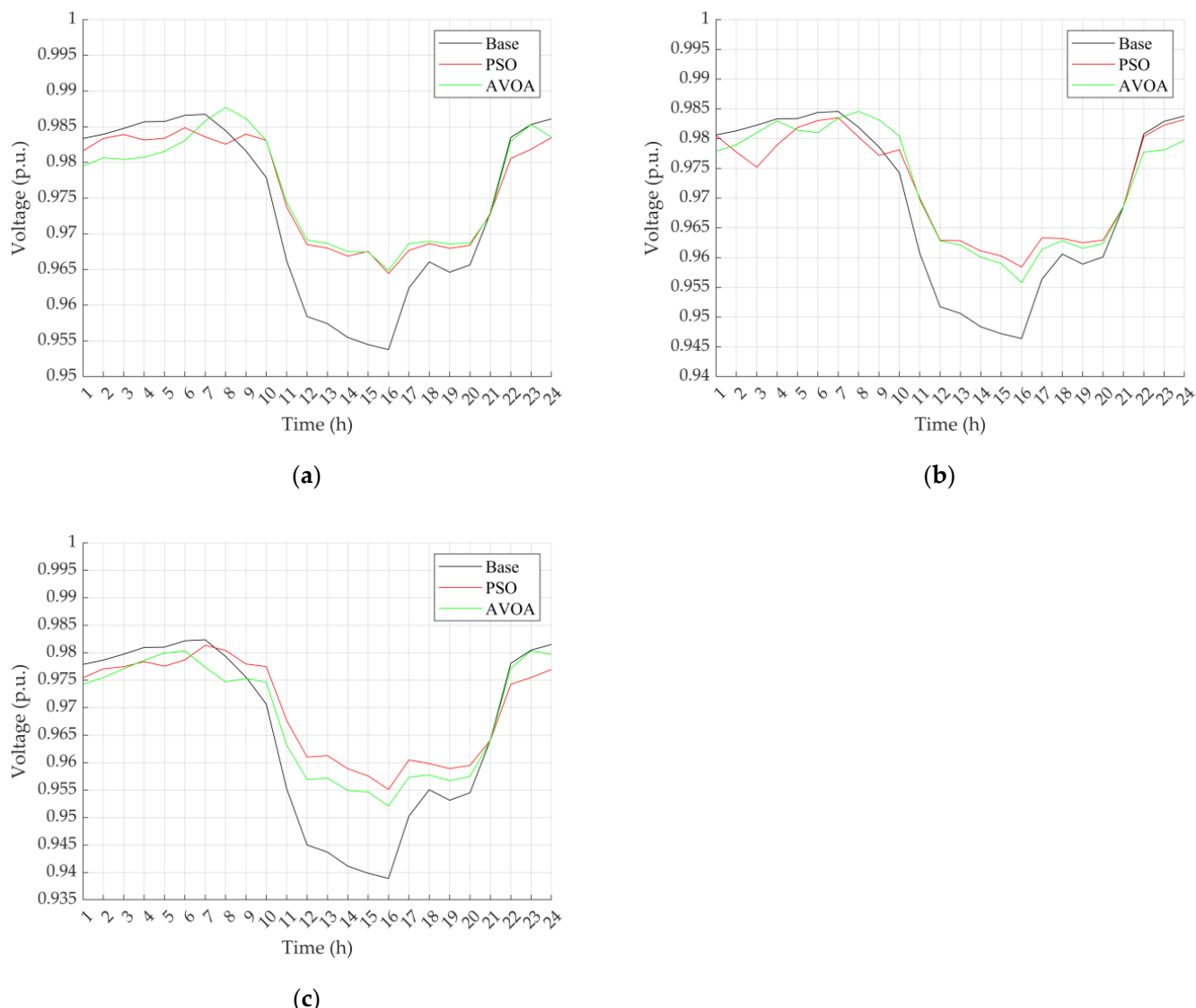
Figure 5. Voltage profile at the 91st bus in the PLA10 distribution system: (**a**) at λ_{ev} 20%; (**b**) at λ_{ev} 40%; (**c**) at λ_{ev} 60%.

The 24-h real line losses in the PLA10 before and after installing the BESS for 20%, 40%, and 60% of EV penetrations provided by PSO and AVOA are plotted in Figure 6.

It can be seen in Figure 6 that the BESS was charging to reserve power to reduce the peak power during the peak period, resulting in the transmission line loss increasing, which was more than the base case in some periods from around 1.00 a.m. to 10.00 a.m. and 9.00 p.m. to 12.00 a.m. However, there was a noticeable drop in transmission loss between 10.00 a.m. and 9.00 p.m. because the BESS discharged power to assist in supplying the network's demand, as evident in Table 4. So, the installation of the BESS and PV enhanced the 24-h transmission line loss when compared to the base case.

Finally, the peak demands in the PLA10 for 20%, 40%, and 60% of EV penetrations before and after installing the BESS and PV by PSO and AVOA are plotted in Figure 7.

(**a**)

(**b**)

(**c**)
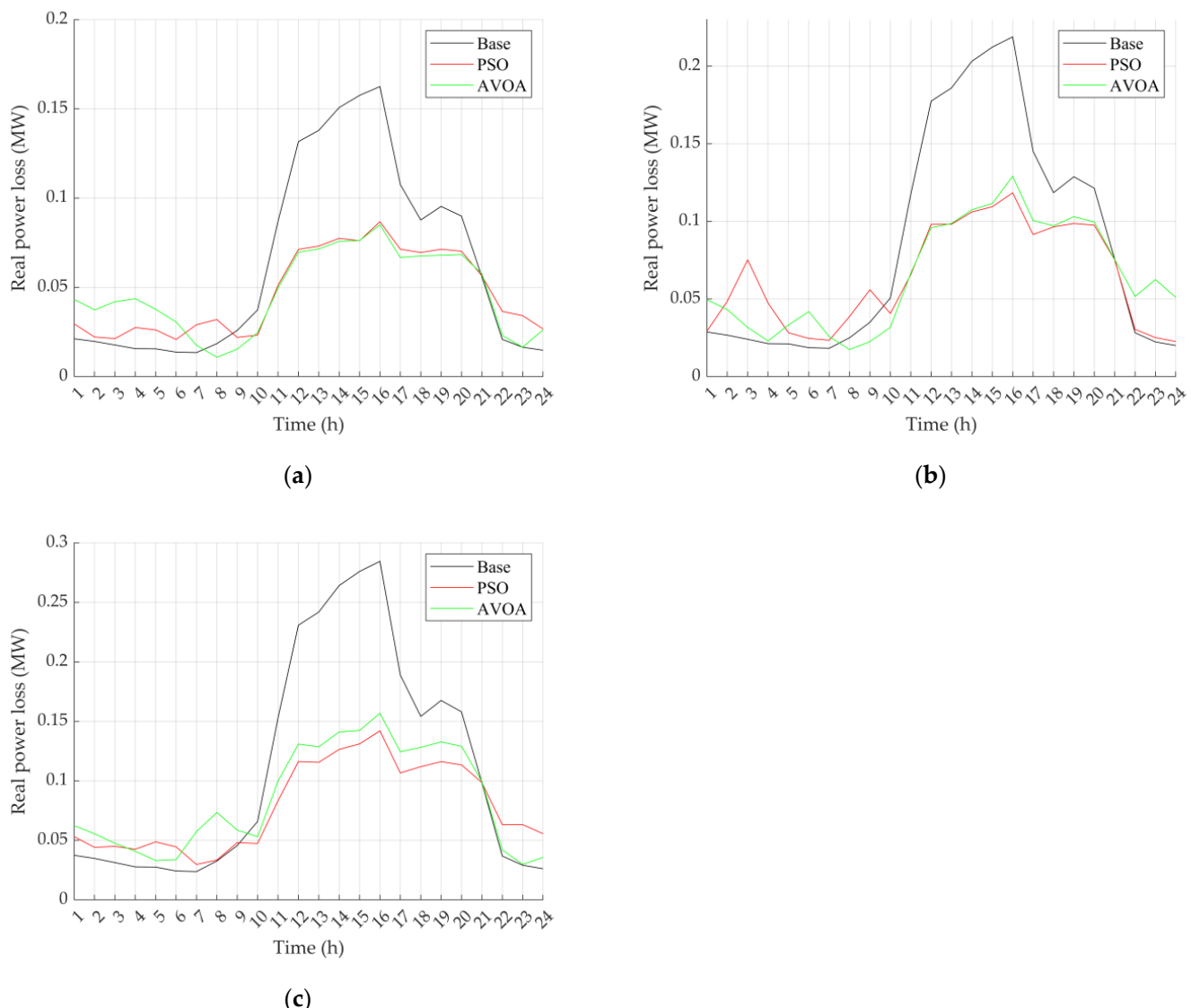
Figure 6. Real power loss in the PLA10 distribution system: (**a**) at λ_{ev} 20%; (**b**) at λ_{ev} 40%; (**c**) at λ_{ev} 60%.

It can be observed from Figure 7 that the peak demand was at 4.00 p.m. for the base case. It is also evident that, following the BESS installation, there were times between 1:00 a.m. and 10:00 a.m. and 9.00 p.m. and 12:00 a.m. when the peak demand exceeded that of the base case because the BESS was charging in order to store energy to lower the peak demand during the highest peak period. Thus, as shown in Table 4, the peak demand was greatly reduced from 10:00 a.m. to 9.00 p.m. following the installation of the BESS, resulting in a 24-h peak demand decrease.

5.2.3. Statistical Analysis and Algorithm Performance Comparison

The statistical results of the considered algorithms are investigated, and the performance of the algorithms is compared. The statistical results and operation times of each algorithm for 20%, 40%, and 60% of EV penetrations are given in Table 5, and the convergence curves of PSO and AVOA for solving the system costs for 20%, 40%, and 60% of EV penetrations are potted in Figure 8.

(**a**)

(**b**)

(**c**)
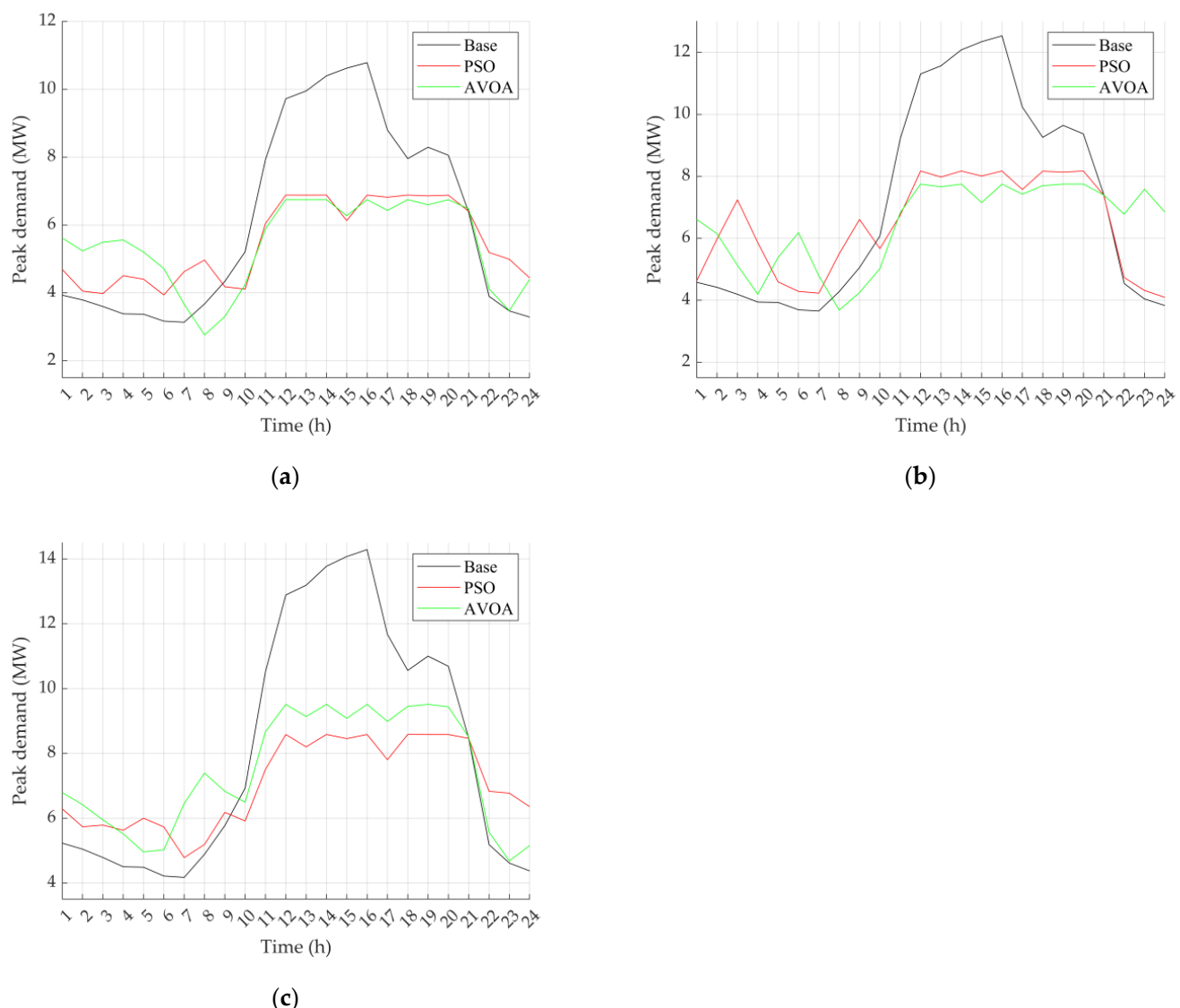
Figure 7. Peak demand in the PLA10 distribution system: (**a**) at λ_{ev} 20%; (**b**) at λ_{ev} 40%; (**c**) at λ_{ev} 60%.

Table 5. Statistical results of each algorithm in the PLA10 distribution system.

Algorithm	λ_{ev}	Best	Worst	Mean	Median	Std.
	20%	40,208,157.04	40,476,376.40	40,369,678.50	40,397,090.20	99,605.69
PSO	40%	47,213,163.04	47,313,442.33	47,254,287.65	47,236,257.59	42,878.09
	60%	54,148,223.67	54,333,070.57	54,229,925.23	54,208,481.46	76,971.73
	20%	40,2831,38.35	40,814,701.71	40,487,523.12	40,466,871.68	198,660.95
AVOA	40%	47,234,023.75	47,750,305.34	47,464,793.62	47,410,051.78	214,296.01
	60%	54,435,077.17	55,431,002.91	54,761,252.60	54,599,970.51	347,863.18

It can be seen from Table 5 that PSO provided the best results in terms of the best value, worst value, mean, median, and standard deviation. From Figure 8, it is noted that the convergence curves generated by both algorithms were very close to each other where both PSO and AVOA took turns converging faster towards the optimal solution.
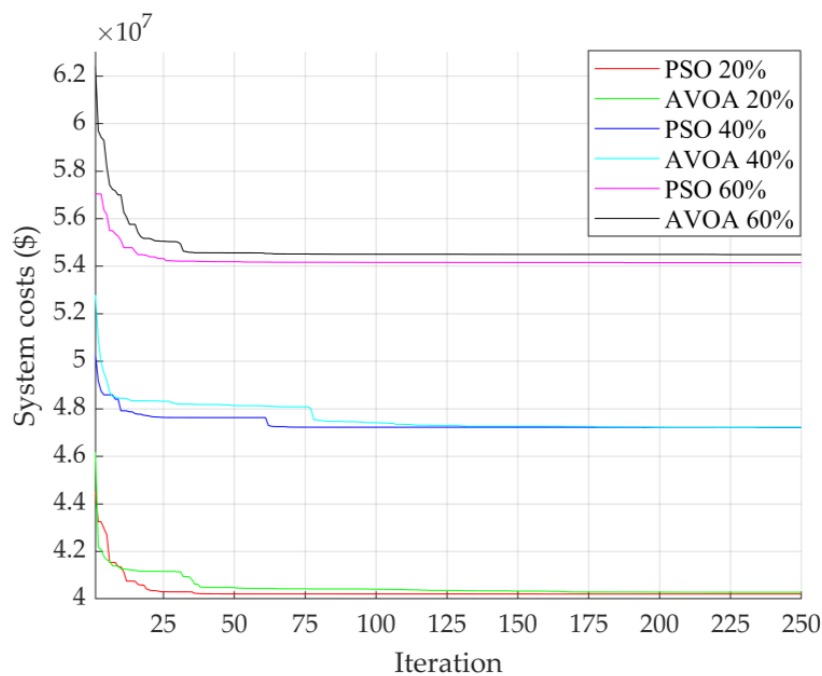
Figure 8. Convergence curves of each algorithm in the PLA10 distribution system at λ_{ev} 20%, 40%, and 60%.

For investment considerations, the calculation of the break-even point involved dividing the costs of installing BESS and PV by the difference between the system's operation and maintenance costs before and following the BESS and PV installations as presented in Table 6.

Table 6. Break-even point of each algorithm.

Algorithm	λ_{ev}	System Costs ($)	Operation and Maintenance Costs for 1 Day ($)	Payback (Years)
Base	20%	-	6345.0331	-
	40%	-	7454.8843	-
	60%	-	8594.2133	-
PSO	20%	40,208,157.04	4095.3141	7.8274
	40%	47,213,163.04	4921.6504	7.5551
	60%	54,148,223.67	5245.0794	8.4142
AVOA	20%	40,2831,38.35	4022.0764	8.1893
	40%	47,234,023.75	4697.4262	7.3293
	60%	54,435,077.17	5561.2344	8.4512

Table 6 shows that the optimal installation of the BESS and PV generated by PSO provided a faster payback period than that of AVOA. However, AVOA provided the quickest payback time at 40% of EV penetration because AVOA has a larger BESS size than that of PSO resulting in a bigger reduction in the peak demand, which affects the costs. However, the break-even point is found based on the same behavior of using BESS and PV every day for a period of 20 years, which may change according to usage behavior.

6. Conclusions

This paper proposed an approach to find the optimal placement and capacity of the BESS and PV while minimizing system costs and enhancing the performance of the distribution system integrated with EVs. The system costs, which are the main objective functions, consisting of installation, replacement, transmission loss, voltage regulation,

and peak demand costs, are minimized while satisfying the considered constraints. The metaheuristic algorithms consisting of PSO and AVOA were applied to solve the problem, and the PLA10 distribution network in Thailand was tested. The simulation results showed that the optimal placement and capacity of BESS and PV in PLA10 considering several levels of EV penetrations could be obtained by both algorithms while PSO could provide lower overall system costs than AVOA. The optimal placement of the BESS for the PLA10 was at the 41st bus, which was observed to be suitable for installing the BESS, while the optimal PV location was at the 51st bus, which was found to be inappropriate for installing the PV, but it can be installed at a nearby bus. For the system performance investigation, it is revealed in most cases of EV penetrations that PSO generated better VDI improvement and real loss reductions while AVOA achieved superior peak demand reductions. The VDI could be reduced, at most, by 86.03%, real power loss decreased the most by 0.78 MW, and the largest peak demand reduction reached 5.706 MW compared to those of the case without installing a BESS and PV. It is found that the system performance could be significantly improved after BESS and PV installations, especially in the case of high EV penetration. In the statistical analysis and algorithm performance comparison, PSO obtained the best statistical values including best value, worst value, mean, median, and standard deviation, and PSO also converged to the optimal solutions faster and had a faster payback period than those of AVOA. So, to find the optimal placement and capacity of the BESS and PV in this tested system, PSO should be adopted to provide efficient solutions. However, this work provided the optimal placement and capacity of the BESS and PV in the practical system simulation, so the real location of the system is required to be observed to determine whether the BESS and PV can really be installed. In the future, the optimal placement and capacity of the BESS and PV from this work will be considered for installation in the real PLA10 distribution network in order to improve system efficiency with minimum investment costs. Moreover, the TOU pricing method can be applied, and the energy from the BESS sold back to the grid can be considered in order to more optimally store and consume the energy, resulting in a faster payback period. In addition, the effect of the EV state of charge on the energy demand can be also studied in order to further interpret the BESS behaviors.

Author Contributions: Conceptualization, S.K. and N.P.; methodology, S.K. and N.P.; software, S.K. and N.P.; validation, S.K., S.P. and A.S.; formal analysis, S.K. and N.P.; investigation, S.K. and N.P.; resources, N.P.; data curation, S.K. and N.P.; writing—original draft preparation, S.K.; writing—review and editing, S.K., N.P., S.P. and A.S.; visualization, S.K.; supervision, S.K.; project administration, S.K.; funding acquisition, S.K. All authors have read and agreed to the published version of the manuscript.

Data Availability Statement: The original contributions presented in the study are included in the article, further inquiries can be directed to the corresponding authors.

Conflicts of Interest: The authors declare no conflicts of interest.

Abbreviations

Abbreviations

AHA	artificial hummingbird algorithm
AVOA	African vulture optimization algorithm
BESS	battery energy storage system
COA	coyote optimization algorithm
DG	distribution generator
DMS	distribution management system
DOD	depth of discharge
EMS	energy management system

ESS	energy storage system
EV	electric vehicle
GA	genetic algorithm
GWO	grey wolf optimizer
IC	investment costs
IPV	Interline-PV
LCC	lower life cycle costs
MC	maintenance costs
MCS	Monte Carlo simulation
mFBI	modified forensic-based investigation
MOPSO	multi-objective PSO
NAA	natural aggregation algorithm
O&M	operation and maintenance
PCS	power conversion system
PLA10	the tenth feeder of Phitsanulok substation 1
PSO	particle swarm optimization
PV	photovoltaic
RC	replacement costs
RES	renewable energy source
SA	simulated annealing
SOE	state of energy
SSA	salp swarm algorithm
THD	total harmonic distortion
TLBO	teaching learning-based optimization
TS	tabu search
VDI	voltage deviation index
WT	wind turbine

Nomenclature

symbols

a_0	constant Fourier coefficient
a_n, b_n	Fourier cosine coefficient, Fourier sine coefficient,
C_{iF}	Fourier coefficient vector
C_{iT}	charging and discharging rates in the considered duration
C_I	BESS investment cost
C_{loss}	line loss cost
$C_{O\&M}$	BESS operation and maintenance costs
C_p	peak demand cost
C_{PV}	PV installation cost
C_R	BESS replacement cost
C_{system}	system costs
C_{VR}	voltage regulation cost
$Cycles$	daily cycle of the BESS
$CyclesLife$	nominal life cycles of the Li-ion battery
D	operation days
$DOD_{\max}$	maximum DOD
E_B	energy in the BESS (MWh)
$E_B{}^{\min}$, $E_B{}^{\max}$	minimum and maximum energies of the BESS
ΔE_B	changes in energies in the BESS at two continuous times
N_{bat}	BESS size (kWh)
N_{br}	total number of branches
N_{bus}	total number of buses
N_{pv}	PV size (kW)
n	number of Fourier coefficients
P_B	BESS power
$P_B{}^{\min}$, $P_B{}^{\max}$	minimum and maximum powers of the BESS
$P^t{}_{cha}$, $P^t{}_{dis}$	charging and discharging of the BESS at a time t

P_D	power of the load demand
$P^t_{d(n)}$, $Q^t_{d(n)}$	total active and reactive power loads integrating EV penetration at the nth bus
$P^0_{ev(n)}$, $Q^0_{ev(n)}$	additional active and reactive loads by the EV penetrations at the nth bus
P_{grid}	power of the grid
$P^0_{L(n)}$, $Q^0_{L(n)}$	nominal active and reactive load power at the nth bus
P^t_L, Q^t_L	active and reactive power losses of line l at each time t
P_L	real loss in each line
P_{loss}	active power loss for each period T
P_{max}	maximum power demand
P_{pv}	power of the PV
Q	lifespan of the BESS in years
Q_{loss}	reactive power loss for each period T
S_{loss}	apparent power loss for each period T
T	total period
t	time
t_{year}	study duration
Δt	sampling interval time
V_i	voltage at the ith bus (p.u.)
V_{min}, V_{max}	minimum and maximum voltages of each bus
V_{ref}	reference voltage
$V^t_{(n)}$, $V^0_{(n)}$	time and initial nominal voltages
%VDI	total percentage of VDI in the system
%VDI_i	maximum percentage of VDI at bus i for each period T
$\alpha\beta$	active and reactive power exponents of the load demand
α_{ev}, β_{ev}	active and reactive power exponents of the EV load demand
γ_I, γ_{VR}, γ_{loss}, γ_p, γ_{pv}	rates of the BESS installation cost, voltage regulation cost, transmission loss cost, maximum energy demand cost and PV installation cost
η_{bat}	cycle efficiency of BESS
η_c, η_d	Charging and discharging efficiencies of the BESS
λ_{ev}	scale factor
$\varphi_{n(c)}$	AC/DC converter power factor
symbols for PSO	
c_1, c_2	positive constant values
g_{best}	best position of the entire particle (global best)
$iter_{max}$	maximum iteration
k	iteration
$p_{best,i}$	best position of the particle i (personal best)
r_1, r_2	random values between 0 and 1
v_i	velocity of particle i
w	inertia weight
w_{max}, w_{min}	maximum and minimum inertia weight
x_i	position of particle i
symbols for AVOA	
A_1, A_2	rivalries for food
$BestVulture_1(i)$, $BestVulture_2(i)$	best vulture of the first and second groups at iteration i
D	parameter adopted to update the best vulture positions in two groups
d	distance of the vulture from one of the best vultures in two groups
F	starvation rate of the vultures
h	number randomly chosen between -2 and 2
i	iteration
L_1, L_2	indicators determined before the searching process
$Levy(d)$	Levy flight
n	number of vulture groups
P	vector of the vulture position
p_i	probability of selecting the best solution
R	one of best vultures

$rand_1, rand_2,$ $rand_3, rand_4,$ $rand_5, rand_6$		random number between 0 and 1
S_1, S_2		spiral equation obtained between all vultures and one of the best vultures in two groups
t		parameter used to enhance the searching operation
ub, lb		variable upper and lower bounds
w		parameter used to balance exploration and exploitation phases
X		movement of vultures randomly move to protect food from others
z		number randomly generated between -1 and 1

Appendix A

The system data of the PLA10 distribution system are presented in Table A1.

Table A1. System data of the PLA10 distribution system.

From Bus	To Bus	Transmission Line		Load at Receiving Bus	
		Resistance (p.u.)	Reactance (p.u.)	Active Power (MW)	Reactive Power (MVar)
1	2	0.00066753	0.00131316	0.040000	0.040000
2	3	0.00304984	0.00599965	0.080000	0.050000
3	4	0.03190178	0.06275724	0	0
4	5	0.00615880	0.01211575	0.000170	0.002000
5	6	0.00416107	0.00818577	0.000160	0.002000
6	7	0.04335671	0.09034338	0.040000	0.030000
7	8	0.08122618	0.18842561	0	0
8	9	0.01395848	0.03238038	0.010000	0.010000
9	10	0.00213025	0.00494169	0	0
10	11	0.04919453	0.11411968	0	0
10	60	0.00384937	0.00757257	3.008000	1.864000
11	12	0.00912894	0.02117700	0.000160	0.003400
11	62	0.02639606	0.05192700	0.804000	0.498200
12	13	0.01396787	0.03240218	0	0
13	14	0.00314541	0.00729661	0.381700	0.023600
13	65	0.01438785	0.00797073	0.014620	0.016500
14	15	0.00615577	0.01427993	0.000160	0.002050
15	16	0.04016105	0.09316418	0	0
16	17	0.00439902	0.01020468	0.000160	0.001030
17	18	0.02003538	0.04647736	0.005770	0.005510
18	19	0.09222763	0.21394636	0.005570	0.038620
19	20	0.06495031	0.15066940	0.178560	0.121240
20	21	0.02132539	0.04946987	0	0
21	22	0.01916562	0.04445972	0.028680	0.023040
21	66	0.15693050	0.06482364	0.090740	0.063640
22	23	0.00740378	0.01717504	0.086560	0.064230
23	24	0.01236938	0.02869405	0.021610	0.018740
24	25	0.06179254	0.14487545	0.003180	0.001976
25	26	0.00572173	0.01327308	0.007210	0.006480
26	27	0.00073966	0.00171583	0	0
27	28	0.00213266	0.00494727	0.147400	0.104600
27	68	0.09849954	0.19377077	0	0
28	29	0.01063023	0.02465962	0.007530	0.004660
29	30	0.01916156	0.04445031	0	0.320350
30	31	0.01916156	0.04445031	0	0
31	32	0.01198843	0.02781033	0.203700	0.134600
31	71	0.00393335	0.00162476	0.168000	0.104100
32	33	0.01265207	0.02934982	0.004640	0.003810

Table A1. *Cont.*

From Bus	To Bus	Transmission Line		Load at Receiving Bus	
		Resistance (p.u.)	Reactance (p.u.)	Active Power (MW)	Reactive Power (MVar)
33	34	0.04567201	0.10594830	0.016490	0.011470
34	35	0.03290951	0.07634231	0	0
35	36	0.04224496	0.09642051	0.001760	0.001090
36	37	0.05730026	0.11272252	0.005335	0.003306
37	38	0.06691377	0.13163447	0.000584	0.000362
38	39	0.01909708	0.03756826	0.000160	0.001000
39	40	0.14006092	0.27553140	0.006120	0.004730
40	41	0.00481246	0.00946720	0	0
41	42	0.06041173	0.11884350	0	0
41	74	0.00490924	0.00202787	0.807000	0.500000
42	43	0.02607389	0.05129321	0.000400	0.003450
42	78	0.02676599	0.01105629	0.000436	0.000270
43	44	0.26283988	0.51706521	0	0
44	45	0.00748726	0.01472912	0.001320	0.000820
45	46	0.01764724	0.03471611	0.008250	0.007050
46	47	0.08322179	0.05876720	0.003240	0.003940
47	48	0.04592143	0.03242749	0	0
48	49	0.03547341	0.01465309	0.004280	0.004510
48	80	0.00871169	0.00359856	0.054010	0.033460
49	50	0.11240115	0.21125256	0	0.311800
50	51	0.00259138	0.00509782	0	0
51	52	0.03175833	0.06247578	0.008020	0.005920
51	82	0.00368953	0.00725813	2.419000	1.499000
52	53	0.09577148	0.18840408	0	0
53	54	0.13929892	0.27403234	0.000340	0.002130
53	83	0.08478230	0.03502123	0	0
54	55	0.03304137	0.06499981	0.000160	0.000970
55	56	0.01455318	0.02862939	0	0
56	57	0.11294182	0.22218196	0.004380	0.002718
57	58	0.00454544	0.00894190	0	0
58	88	0.13124128	0.05421213	0.011150	0.006910
58	59	0.11447834	0.22728361	0.007940	0.005870
60	61	0.00227225	0.00447004	0.000980	0.196900
62	63	0.01036553	0.02039132	0.000160	0.027130
63	64	0.00243037	0.00478109	0.000160	0.027130
66	67	0.03859241	0.01594146	0.007620	0.009990
68	69	0.01777059	0.03495874	0.000160	0.003370
69	70	0.20185744	0.15214860	0.008380	0.519700
71	72	0.00347006	0.00143339	0.000160	0.021290
72	73	0.01266308	0.00998547	0.000160	0.013420
74	75	0.00438857	0.00181280	0.000160	0.021030
75	76	0.01184211	0.00489165	0.000160	0.020900
76	77	0.00909933	0.00375868	0.000160	0.021030
78	79	0.02405394	0.01813048	0.015400	0.009580
80	81	0.00446599	0.00184478	0.008000	0.015260
83	84	0.01456305	0.00601559	0.040970	0.030930
83	86	0.03047604	0.01258881	0.039520	0.030000
84	85	0.09970403	0.04118499	0.042040	0.031610
86	87	0.15245500	0.06297496	0.007440	0.009720
88	89	0.02513544	0.01038276	0	0
89	90	0.01389884	0.00574123	0.004320	0.002680
89	91	0.06395522	0.02641814	0.015780	0.009780

References

1. Raihan, A.; Tuspekova, A. Dynamic Impacts of Economic Growth, Energy Use, Urbanization, Tourism, Agricultural Value-Added, and Forested Area on Carbon Dioxide Emissions in Brazil. *J. Environ. Stud. Sci.* **2022**, *12*, 794–814. [CrossRef]
2. Hassan, M.S.; Mahmood, H.; Javaid, A. The Impact of Electric Power Consumption on Economic Growth: A Case Study of Portugal, France, and Finland. *Environ. Sci. Pollut. Res.* **2022**, *29*, 45204–45220. [CrossRef] [PubMed]
3. Kongkuah, M.; Yao, H.; Yilanci, V. The Relationship between Energy Consumption, Economic Growth, and CO_2 Emissions in China: The Role of Urbanisation and International Trade. *Environ. Dev. Sustain.* **2022**, *24*, 4684–4708. [CrossRef]
4. Dai, Q.; Liu, J.; Wei, Q. Optimal Photovoltaic/Battery Energy Storage/Electric Vehicle Charging Station Design Based Onmulti-Agent Particle Swarm Optimization Algorithm. *Sustainability* **2019**, *11*, 1973. [CrossRef]
5. Motalleb, M.; Reihani, E.; Ghorbani, R. Optimal Placement and Sizing of the Storage Supporting Transmission and Distribution Networks. *Renew. Energy* **2016**, *94*, 651–659. [CrossRef]
6. El-Batawy, S.A.; Morsi, W.G. Optimal Design of Community Battery Energy Storage Systems with Prosumers Owning Electric Vehicles. *IEEE Trans. Industr. Inform.* **2018**, *14*, 1920–1931. [CrossRef]
7. Kamel, O.M.; Abdelaziz, A.Y.; Zaki Diab, A.A. Damping Oscillation Techniques for Wind Farm DFIG Integrated into Inter-Connected Power System. *Electr. Power Compon. Syst.* **2020**, *48*, 1551–1570. [CrossRef]
8. Kamel, O.M.; Diab, A.A.Z.; Mahmoud, M.M.; Al-Sumaiti, A.S.; Sultan, H.M. Performance Enhancement of an Islanded Microgrid with the Support of Electrical Vehicle and STATCOM Systems. *Energies* **2023**, *16*, 1577. [CrossRef]
9. Tovilović, D.M.; Rajaković, N.L.J. The Simultaneous Impact of Photovoltaic Systems and Plug-in Electric Vehicles on the Daily Load and Voltage Profiles and the Harmonic Voltage Distortions in Urban Distribution Systems. *Renew. Energy* **2015**, *76*, 454–464. [CrossRef]
10. Babacan, O.; Torre, W.; Kleissl, J. Siting and Sizing of Distributed Energy Storage to Mitigate Voltage Impact by Solar PV in Distribution Systems. *Sol. Energy* **2017**, *146*, 199–208. [CrossRef]
11. Das, C.K.; Bass, O.; Kothapalli, G.; Mahmoud, T.S.; Habibi, D. Overview of Energy Storage Systems in Distribution Networks: Placement, Sizing, Operation, and Power Quality. *Renew. Sustain. Energy Rev.* **2018**, *91*, 1205–1230. [CrossRef]
12. Desai, B.G. *Electrical Energy Storage*; White Paper; IEC: Geneva, Switzerland, 1981; Volume 1. [CrossRef]
13. Fathy, A. A Novel Artificial Hummingbird Algorithm for Integrating Renewable Based Biomass Distributed Generators in Radial Distribution Systems. *Appl. Energy* **2022**, *323*, 119605. [CrossRef]
14. Boonluk, P.; Siriratratiwat, A.; Fuangfoo, P.; Khunkitti, S. Optimal Siting and Sizing of Battery Energy Storage Systems for Distribution Network of Distribution System Operators. *Batteries* **2020**, *6*, 56. [CrossRef]
15. Tolba, M.A.; Houssein, E.H.; Eisa, A.A.; Hashim, F.A. Optimizing the Distributed Generators Integration in Electrical Distribution Networks: Efficient Modified Forensic-Based Investigation. *Neural Comput. Appl.* **2023**, *35*, 8307–8342. [CrossRef]
16. Mazza, A.; Mirtaheri, H.; Chicco, G.; Russo, A.; Fantino, M. Location and Sizing of Battery Energy Storage Units in Low Voltage Distribution Networks. *Energies* **2019**, *13*, 52. [CrossRef]
17. Jayasekara, N.; Masoum, M.A.S.; Wolfs, P.J. Optimal Operation of Distributed Energy Storage Systems to Improve Distribution Network Load and Generation Hosting Capability. *IEEE Trans. Sustain. Energy* **2016**, *7*, 250–261. [CrossRef]
18. Khalid, M.; Akram, U.; Shafiq, S. Optimal Planning of Multiple Distributed Generating Units and Storage in Active Distribution Networks. *IEEE Access* **2018**, *6*, 55234–55244. [CrossRef]
19. Zheng, Y.; Song, Y.; Huang, A.; Hill, D.J. Hierarchical Optimal Allocation of Battery Energy Storage Systems for Multiple Services in Distribution Systems. *IEEE Trans. Sustain. Energy* **2020**, *11*, 1911–1921. [CrossRef]
20. Ahmadian, A.; Sedghi, M.; Aliakbar-Golkar, M. Fuzzy Load Modeling of Plug-in Electric Vehicles for Optimal Storage and DG Planning in Active Distribution Network. *IEEE Trans. Veh. Technol.* **2017**, *66*, 3622–3631. [CrossRef]
21. Sadeghi, D.; Hesami Naghshbandy, A.; Bahramara, S. Optimal Sizing of Hybrid Renewable Energy Systems in Presence of Electric Vehicles Using Multi-Objective Particle Swarm Optimization. *Energy* **2020**, *209*, 118471. [CrossRef]
22. Janamala, V.; Sreenivasulu Reddy, D. Coyote Optimization Algorithm for Optimal Allocation of Interline –Photovoltaic Battery Storage System in Islanded Electrical Distribution Network Considering EV Load Penetration. *J. Energy Storage* **2021**, *41*, 102981. [CrossRef]
23. Khunkitti, S.; Boonluk, P.; Siriratratiwat, A. Optimal Location and Sizing of BESS for Performance Improvement of Distribution Systems with High DG Penetration. *Int. Trans. Electr. Energy Syst.* **2022**, *2022*, 1–16. [CrossRef]
24. Pompern, N.; Premrudeepreechacharn, S.; Siriratratiwat, A.; Khunkitti, S. Optimal Placement and Capacity of Battery Energy Storage System in Distribution Networks Integrated With PV and EVs Using Metaheuristic Algorithms. *IEEE Access* **2023**, *11*, 68379–68394. [CrossRef]
25. Mclarnon, F.R.; Cairns, E.J. Energy Storage. *Annu. Rev. Energy* **1989**, *14*, 241–271. [CrossRef]
26. Kousksou, T.; Bruel, P.; Jamil, A.; El Rhafiki, T.; Zeraouli, Y. Energy Storage: Applications and Challenges. *Sol. Energy Mater. Sol. Cells* **2014**, *120*, 59–80. [CrossRef]
27. Yekini Suberu, M.; Wazir Mustafa, M.; Bashir, N. Energy Storage Systems for Renewable Energy Power Sector Integration and Mitigation of Intermittency. *Renew. Sustain. Energy Rev.* **2014**, *35*, 499–514. [CrossRef]
28. Stecca, M.; Ramirez Elizondo, L.; Batista Soeiro, T.; Bauer, P.; Palensky, P. A Comprehensive Review of the Integration of Battery Energy Storage Systems into Distribution Networks. *IEEE Open J. Ind. Electron. Soc.* **2020**, *1*, 46–65. [CrossRef]

29. Boonluk, P.; Khunkitti, S.; Fuangfoo, P.; Siritaratiwat, A. Optimal Siting and Sizing of Battery Energy Storage: Case Study Seventh Feeder at Nakhon Phanom Substation in Thailand. *Energies* **2021**, *14*, 1458. [CrossRef]

30. Wolfs, P.; Jayasekera, N.; Subawickrama, S. A Fourier Series Based Approach to the Periodic Optimisation of Finely Dispersed Battery Storage. In Proceedings of the AUPEC 2011, Brisbane, QLD, Australia, 25–28 September 2011; pp. 1–6.

31. Satyanarayana, S.; Ramana, T.; Sivanagaraju, S.; Rao, G.K. An Efficient Load Flow Solution for Radial Distribution Network Including Voltage Dependent Load Models. *Electr. Power Compon. Syst.* **2007**, *35*, 539–551. [CrossRef]

32. Abualigah, L.; Altalhi, M. A Novel Generalized Normal Distribution Arithmetic Optimization Algorithm for Global Optimization and Data Clustering Problems. *J. Ambient. Intell. Humaniz. Comput.* **2024**, *15*, 389–417. [CrossRef]

33. Chen, X.; Ding, K.; Zhang, J.; Yang, Z.; Liu, Y.; Yang, H. A Two-Stage Method for Model Parameter Identification Based on the Maximum Power Matching and Improved Flow Direction Algorithm. *Energy Convers. Manag.* **2023**, *278*, 116712. [CrossRef]

34. Eberhart, R.; Kennedy, J. A New Optimizer Using Particle Swarm Theory. In Proceedings of the MHS'95. Proceedings of the Sixth International Symposium on Micro Machine and Human Science, Nagoya, Japan, 4–6 October 1995; IEEE: Piscataway, NJ, USA, 1995; pp. 39–43.

35. Abdollahzadeh, B.; Gharehchopogh, F.S.; Mirjalili, S. African Vultures Optimization Algorithm: A New Nature-Inspired Metaheuristic Algorithm for Global Optimization Problems. *Comput. Ind. Eng.* **2021**, *158*, 107408. [CrossRef]

36. MATPOWER—Free, Open-Source Tools for Electric Power System Simulation and Optimization. Available online: https://matpower.org/ (accessed on 30 April 2024).